Pharmaceutical Research, Vol. 26, No. 10, October 2009 (© 2009)
DOI: 10.1007/s11095-009-9946-7

Research Paper

A Quantitative Kinetic Study of Polysorbate Autoxidation: The Role of Unsaturated Fatty Acid Ester Substituents

Jia Yao,[1,2] Dushyanth K. Dokuru,[1] Matthew Noestheden,[1] SungAe S. Park,[3] Bruce A. Kerwin,[4] Janan Jona,[1] Drazen Ostovic,[1] and Darren L. Reid[1,5]

Received May 1, 2009; accepted July 14, 2009; published online August 8, 2009

Purpose. To study the role of unsaturated fatty acid ester substituents in the autoxidation of polysorbate 80 using quantitative kinetics.
Methods. Oxidation kinetics were monitored at 40°C in aqueous solution by tracking head space oxygen consumption using a fiber optic oxygen sensor with phase shift fluorescence detection. Radical chain initiation was controlled using an azo-initiator and assessed by Hammond's inhibitor approach, allowing oxidizability constants ($k_p/(2k_t)^{1/2}$) to be isolated. Reaction orders were determined using modified van't Hoff plots and mixed polysorbate micelles.
Results. The oxidizability constant of polysorbate 80 ($(1.07\pm0.19)\times10^{-2}$ $M^{-1/2}$ $s^{-1/2}$) was found to be 2.65 times greater than polysorbate 20 ($(0.404\pm0.080)\times10^{-2}$ $M^{-1/2}$ $s^{-1/2}$). The additional reactivity of polysorbate 80 was isolated and was first-order in the unsaturated fatty acid ester substituents, indicating that the bulk of the autoxidative chain propagation is due to these groups. This data, and the observation of a half-order dependence on the azo-initiator, is consistent with the classical autoxidation rate law ($-d[O_2]/dt = k_p[RH](R_i/2k_t)^{1/2}$).
Conclusions. Polysorbate 80 autoxidation follows the classical rate law and is largely dependent on the unsaturated fatty acid ester substituents. Clarification of the substituents' roles will aid formulators in the selection of appropriate polysorbates to minimize oxidative liabilities.

KEY WORDS: autoxidation; kinetics; micelle; oxidation; polysorbate.

INTRODUCTION

Polysorbates are an important class of amphipathic, nonionic, surfactants that are widely used in pharmaceuticals in clinical and preclinical settings due to their broad applicability and low toxicities (1,2). In the formulation of proteins, they are used as surfactants to prevent surface adsorption, limiting physical damage during purification, filtration, transportation, freeze-drying, spray drying, storage, and delivery (1). In small molecule pharmaceutics, they are used in clinical and preclinical settings as emulsifying, solubilizing and wetting agents, depending on the concentrations used (3–6). Polysorbate 80 (PS-80—polyoxyethylene sorbitan monooleate) and Polysorbate 20 (PS-20—polyoxyethylene sorbitan monolaurate) are the most common polysorbates used in the formulation of small molecule and protein biopharmaceuticals, and their physical and chemical properties have been reviewed recently (1,3,4). They are composed of fatty acid esters of polyoxyethylene sorbitan, and their structures are typically presented as the chemically homogenous polysorbates shown in Fig. 1. Both PS-20 and PS-80 have a common sorbitan ring backbone, and hydrophilic character is provided

[1] Amgen, Inc., Pharmaceutical Research and Development, Thousand Oaks, California, USA.
[2] *Present Address:* Amgen, Inc., Analytical Research and Development, Thousand Oaks, California, USA.
[3] Amgen, Inc., Formulation & Analytical Resources, Thousand Oaks, California, USA.
[4] Amgen, Inc., Analytical & Formulation Sciences, Seattle, Washington, USA.
[5] To whom correspondence should be addressed. (e-mail: dreid@amgen.com)

ABBREVIATIONS: AAPH, 2,2′-azobis-2-methyl-propanimidamide, dihydrochloride; API, Active pharmaceutical ingredient; CMC, Critical micelle concentration; $d[O_2]/dt$, Rate of oxygen uptake; *e*, Efficiency factor; EDTA, Ethylenediaminetetraacetic acid; k_i, Initiation rate constant; k_p, Propagation rate constant; $k_p/(2k_t)^{1/2}$, Oxidizability constant; k_{p1}, Propagation rate constant for fatty acid ester substituents; k_{p2}, Propagation rate constant for ethylene oxide substituents; PS-20, Polysorbate 20, polyoxyethylene sorbitan monolaurate; PS-80, Polysorbate 80, polyoxyethylene sorbitan monooleate; R_i, Initiation rate; ROS, Reactive oxygen species; R_p, Propagation rate; R_t, Termination rate; Trolox, 6-hydroxy-2,5,7,8-tetramethyl chroma-2-carboxylic acid; τ, Inhibition time; $2k_t$, Termination rate constant; $2k_{t1}$, Termination rate constant for fatty acid ester autoxidation; $2k_{t2}$, Termination rate constant for ethylene oxide autoxidation.

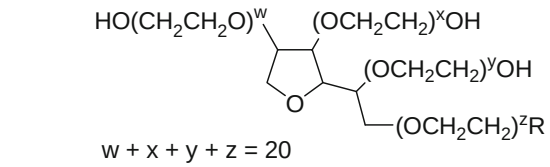

Polysorbate 20 - polyoxyethylene sorbitan monolaurate:

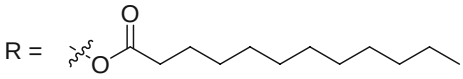

Polysorbate 80 - polyoxyethylene sorbitan monooleate:

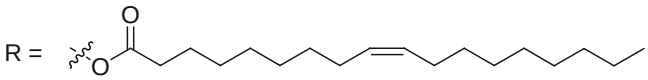

Fig. 1. Chemical structures of polysorbate 20 and polysorbate 80.

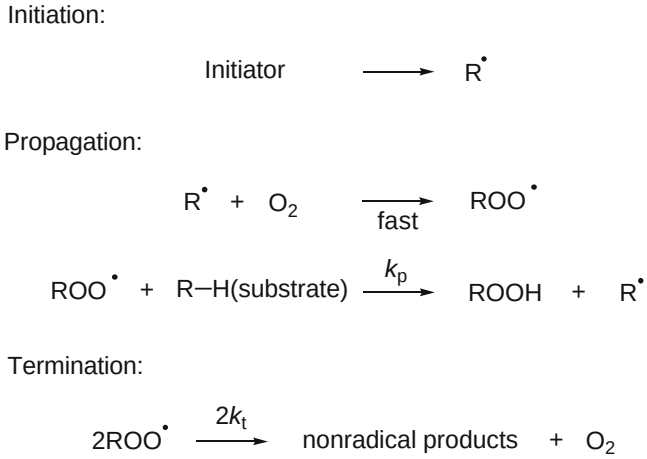

Fig. 2. General autoxidation mechanism.

by the ethylene oxide polymer subunits attached at four different hydroxyl positions. PS-20 and PS-80 only differ in the structures of the fatty acid ester side chains attached to one of the ethylene oxide subunits, which provide the hydrophobic nature of these surfactants. While the number of repeat ethylene oxide subunits varies at each position, their total number (w + x + y + z, Fig. 1) equals 20 and is constant for each polysorbate. The fatty acid ester moieties are attached through an ester linkage to the ethylene oxide oxygen at the z position. The laurate moiety of PS-20 is a saturated straight chain hydrocarbon, and the oleate moiety of PS-80 is unsaturated, containing a double-bond, resulting in a kink in the hydrocarbon chain. Commercially available polysorbates are generally chemically diverse mixtures of different fatty acid esters (7–9). While the European Pharmacopoeia specifies the composition of the fatty acid ester substituents for PS-20 and PS-80, as summarized in Table I (10), the United States Pharmacopoeia does not define the percentage of fatty acid esters in polysorbates (10,11). Analysis of polysorbates from different vendors using reverse phase HPLC coupled with a charged aerosol detector has shown only minor differences in the fatty acid ester contents (1).

Whenever polysorbates are used in formulations, the chemical stability of the active pharmaceutical ingredient (API) must be addressed due to their ability to promote oxidation (12–17). Polysorbates are susceptible to autoxidation, resulting in the formation of high concentrations of reactive oxygen species (ROS), which can oxidize APIs. Underscoring this point, PS-80 has been used as an oxidizing reagent for the assessment of drug stability (18). The general mechanism of autoxidation of most organic substrates in solution is a free-radical chain process which, at oxygen partial pressures above ca. 13.3 kPa, can be represented by the reaction sequence shown in Fig. 2 (19–22). In this process an alkyl radical is formed in the initiation step. This may occur by various processes, including thermal or photochemical homolytic cleavage of an RH bond, resulting in the formation of a peroxyl radical by a fast, diffusion-controlled reaction with O_2. The peroxyl radicals can propagate the radical chain reactions through hydrogen atom abstraction from reactive C-H groups or, alternatively, by participating in radical chain terminating steps, producing non-radical products and O_2. The rate constants for radical chain propagation (k_p) and chain termination ($2k_t$) are key to understanding the susceptibility of a given substrate to oxidation.

The oxidation mechanism of polysorbates was first described by Donbrow *et al.* based on their seminal work with PS-20 (12,23,24). PS-20 oxidation was studied by monitoring the formation of peroxides, changes in acidity, and the generation of organic acids and other products. The results were consistent with the autoxidation of the ethylene oxide moieties, resulting in Eq. 1 as the overall propagation

Table I. Composition of the Fatty Acid Ester Substituents of PS-20 and PS-80 and the Corresponding Acid Structures

	EU specifications		
Acid	PS-20	PS-80	Structure
Caproic	≤1%		$CH_3(CH_2)_4COOH$
Caprylic	≤10%		$CH_3(CH_2)_6COOH$
Capric	≤10%		$CH_3(CH_2)_8COOH$
Lauric	40–60%		$CH_3(CH_2)_{10}COOH$
Myristic	14–25%	≤5%	$CH_3(CH_2)_{12}COOH$
Palmitic	7–15%	≤16%	$CH_3(CH_2)_{14}COOH$
Palmitoleic		≤8%	$CH_3(CH_2)_5CH=CH(CH_2)_7COOH$
Stearic	≤7%	≤6%	$CH_3(CH_2)_{16}COOH$
Oleic	≤11%	≥58%	$CH_3(CH_2)_7CH=CH(CH_2)_7COOH$
Linoleic	≤3%	≤18%	$CH_3(CH_2)_4CH=CHCH_2CH=CH(CH_2)_7COOH$
Linolenic		≤4%	$CH_3CH_2CH=CHCH_2CH=CHCH_2CH=CH(CH_2)_7COOH$

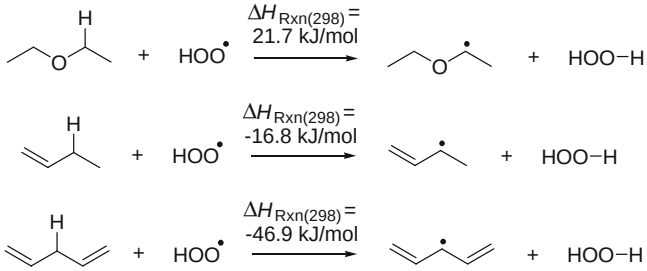

Fig. 3. Heats of reaction for H-atom abstraction by hydroperoxyl radicals.

reaction. In 2002, Ha *et al.* studied the formation of peroxides in PS-80 under various conditions and found that the oxidation of PS-80 resulted in an initial increase in peroxides that could be limited by removing O_2 from the system (2). The results were considered to be consistent with Donbrow's polyoxyethylene chain autoxidation mechanism (12,23,24).

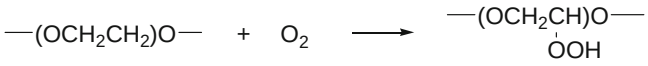

(1)

In addition to the polyoxyethylene groups present in PS-20, PS-80 also contains mono-, di-, and tri-unsaturated fatty acid esters as the primary hydrophobic substituents, which raises the possibility of an additional important oxidative pathway for this surfactant. Oxidation of unsaturated fatty acids is a well-known process, and the possibility that this pathway plays a role in polysorbate autoxidation has undoubtedly been discussed in many informal settings and was recently raised in print by Kerwin (1,25). The basis for suggesting that the unsaturated fatty acid ester substituents could be playing a key role in the autoxidation of polysorbates lies in the relative susceptibility of ethylene oxide hydrogens *vs.* allyl or pentadienyl hydrogens to hydrogen atom abstraction. For example, consider the gas phase hydrogen atom abstraction reactions for diethyl ether, 1-butylene, and 1,4-pentadiene by hydroperoxyl radicals (Fig. 3). The enthalpy of reaction for these transformations can be calculated from the enthalpy of formation for each species (26). Hydrogen abstraction from diethyl ether is calculated to have an enthalpy of reaction of 21.7 kJ/mol and is endothermic. However, the enthalpies of reaction for hydrogen abstraction from 1-butylene and 1,4-pentadiene are exothermic at −16.8 kJ/mol and −46.9 kJ/mol, respectively. Simply based on this thermodynamic analysis, the unsaturated fatty acid ester substituents would be expected to be far more susceptible to autoxidation than ethylene oxide groups. This is compounded by the fact that, in addition to hydrogen atom abstraction, peroxyl radicals can also propagate the oxidation of olefins by direct attack at the double bond, resulting in the formation of oligomeric polyoxides (Fig. 4) (27). This reaction can occur at rates similar to H-atom abstraction as can be seen from oxidation studies where the ratio of addition products (ROOR) to abstraction products (ROOH) has been determined. For example, the ROOR/ROOH product ratios for the oxidation of 1-hexene, 1-butene and cyclohexene are 0.33 (90°C), 0.26 (70°C) and 0.044 (40°C), respectively, indicating that the peroxyl radical addition is also a facile reaction (27). The thermodynamics of H-atom abstraction and the presence of an additional important oxidative pathway suggest that the oxidation of unsaturated fatty acid esters should play an important role in the autoxidation of polysorbates containing these substituents.

This work will explore the possible role of unsaturated fatty acid esters, relative to ethylene oxide substituents, in the autoxidation of PS-80 through the application of quantitative kinetics. The relative reactivities of PS-20 and PS-80 samples to autoxidation will be determined in the form of their classical oxidizability constants, which separate the rate constants for radical chain propagation and termination from the rate constant for radical chain initiation (21). Using van't Hoff's method of kinetic order plots, the dependence of PS-80's autoxidation on the unsaturated fatty acid esters will be determined (28). An improved understanding of the role of the different substituents in polysorbate oxidation will help define strategies to address API oxidation in surfactant formulations and aid in the selection of appropriate polysorbates to minimize oxidative liabilities.

MATERIALS AND METHODS

Kinetic Approach and Data Treatment

Determination of Oxidizability Constants

Quantitative kinetic studies of autoxidation processes require that the rate of radical chain initiation must be known and controlled (19). This was accomplished here using a standard thermal initiator approach under conditions where new radical chains were started only by the decomposition of the initiator, Fig. 5. The rate constant, k_i, for decomposition of the azo-initiator used was determined, as described below, by measuring the loss of azo-initiator by HPLC. However, to derive the rate of radical chain initiation, the rate of radical escape from the solvent cage had to be evaluated, since only the fraction of radicals that diffuse out of the solvent cage are able to initiate autoxidation chains. The inhibitor method, developed by Hammond and co-workers, was used to determine this fraction, or initiator efficiency factor (e) (21). A known concentration of a chain-breaking phenolic antioxidant, ArOH, which has been shown to react with exactly two peroxyl radicals was added to the system, and the inhibition time, τ, during which oxidation was suppressed was measured. The rate of chain initiation, R_i, was then

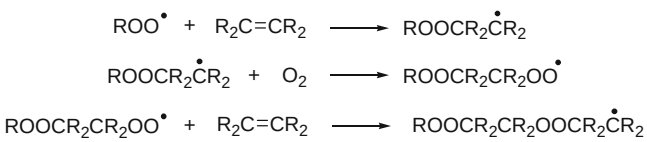

Fig. 4. Addition of peroxyl radicals to double bonds.

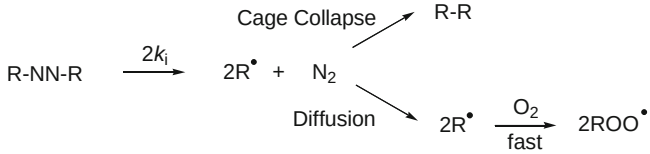

Fig. 5. Controlled initiation by Azo-initators.

determined from τ according to Eq. 2. Knowing the rate of chain initiation allowed the initiator efficiency to be calculated (Eq. 3).

$$\text{Initiation Rate} = \mathrm{R_i} = \frac{2[\text{Inhibitor}]}{\tau} \tag{2}$$

$$\text{Initiator Efficiency}(e) = \frac{\mathrm{R}_i}{2k_i[\text{RNNR}]} \tag{3}$$

At oxygen partial pressures above ca. 13.3 kPa, autoxidation kinetics are zero-order in O_2, and the rate of radical chain propagation, R_p, can be easily related to the rate of O_2 uptake in the system (19–22). From Fig. 2, the rates of propagation and termination are expressed by Eq. 4 and Eq. 5 respectively.

$$\text{Propagation Rate} = \mathrm{R_p} = -\frac{d[\mathrm{O_2}]}{dt} = k_p\left[\mathrm{RO_2^\bullet}\right][\mathrm{R-H}] \tag{4}$$

$$\text{Termination Rate} = \mathrm{R_t} = -\frac{d\left[\mathrm{RO_2^\bullet}\right]}{dt} = 2k_t\left[\mathrm{RO_2^\bullet}\right]^2 \tag{5}$$

The radical chain length, ν, is given by Eq. 6.

$$\text{Chain Length} = \nu = R_p/R_i \tag{6}$$

At steady state $R_i = R_t$, allowing the peroxyl radical concentration, $[RO_2^\bullet]$, to be determined from Eq. 3 and Eq. 5 resulting in Eq. 7. Substituting Eq. 7 into the propagation rate equation (Eq. 4) gives Eq. 8, the classical rate law for autoxidation. Equation 8 can be rearranged to Eq. 9 isolating the key factors that define the susceptibility of a substrate to autoxidation, the propagation and termination rate constants, k_p and $2k_t$. The term, $k_p/(2k_t)^{1/2}$, is known as the oxidizability constant of a substrate and, in this study, is a measure of the relative reactivities of the polysorbates.

$$\left[\mathrm{RO_2^\bullet}\right] = \frac{(e2k_i[\text{RNNR}])^{1/2}}{(2k_t)^{1/2}} = \frac{\mathrm{R_i}^{1/2}}{(2k_t)^{1/2}} \tag{7}$$

$$-\frac{d[\mathrm{O_2}]}{dt} = k_p \times \frac{(e2k_i[\text{RNNR}])^{1/2}}{(2k_t)^{1/2}} \times [\mathrm{R-H}] = k_p \times \frac{\mathrm{R_i}^{1/2}}{(2k_t)^{1/2}} \times [\mathrm{R-H}] \tag{8}$$

$$\text{Oxidizability Constant} = \frac{k_p}{(2k_t)^{1/2}} = \frac{-d[\mathrm{O_2}]/dt}{[\mathrm{R-H}] \times \mathrm{R_i}^{1/2}} \tag{9}$$

Determination of Reaction Orders

Kinetic reaction orders were obtained using van't Hoff's kinetic order plot approach (28). Taking the log of the relevant rate equation and rearranging allows the log of the reaction rate to be plotted against the log of the applicable substrate concentration for a series of reactions. The slope of such a plot yields the reaction order in the substrate for which the concentration is varied.

To investigate the reaction order in the initiator concentration, the log of the classical rate law (Eq. 8) was taken and rearranged to obtain Eq. 10. The polysorbate concentration term, [R-H], was grouped with the left side of the equation to minimize errors due to small differences in concentration in different experimental runs. The slope of this equation, m, is expected to be 0.5.

$$\log\left(-\frac{d[\mathrm{O_2}]/dt}{[R-H]}\right) = m\log[\text{RNNR}] + \log\left(\frac{k_p}{(2k_i)^{1/2}}(e2k_i)^m\right) \tag{10}$$

A kinetic order plot approach was also used to evaluate the possible contribution of the unsaturated fatty acid ester substituents to the autoxidation of PS-80. The fatty acid ester contribution was separated from the ethylene oxide contribution by using mixed micelles of PS-80 and PS-20 to vary the concentration of unsaturated fatty acid esters within the micelles themselves while holding the concentration of ethylene oxide groups constant (1). This was possible since PS-80 and PS-20 have the same number of ethylene oxide groups, but PS-20 has a much lower concentration of unsaturated fatty acid esters. Under these conditions, the substrate concentration term, [R-H], in the propagation rate equation, (Eq. 4) can be taken as the sum of the unsaturated fatty acid ester concentration, $[R\text{-}H_1]$, and the saturated ethylene oxide group concentration $[R\text{-}H_2]$. Defining [R-H] = $[R\text{-}H_1]$ + $[R\text{-}H_2]$ in Eq. 4 gives Eq. 11 where k_{p1} is the total rate constant for unsaturated fatty acid ester H-atom abstraction and double bond addition, and k_{p2} is the rate constant for ethylene oxide H-atom abstraction.

$$\mathrm{R_p} = -\frac{d[\mathrm{O_2}]}{dt} = k_{p1}\left[\mathrm{RO_2^\bullet}\right][\mathrm{R-H_1}]^{\mathrm{m}} + k_{p2}\left[\mathrm{RO_2^\bullet}\right][\mathrm{R-H_2}]^{\mathrm{n}} \tag{11}$$

Substituting for $[RO_2^\bullet]$, from Eq. 7 gives Eq. 12 where k_{t1} and k_{t2} are the termination rate constants for the unsaturated fatty acid ester and ethylene oxide autoxidation reactions, respectively.

$$-\frac{d[\mathrm{O_2}]}{dt} = k_{p1}\frac{(R_i)^{1/2}}{(2k_{t1})^{1/2}}[\mathrm{R-H_1}]^m + k_{p2}\frac{(R_i)^{1/2}}{(2k_{t2})^{1/2}}[\mathrm{R-H_2}]^n \tag{12}$$

The unsaturated fatty acid ester terms can now be isolated on the right-hand side of the equation (Eq. 13). Taking the log gives Eq. 14.

$$\frac{-d[\mathrm{O_2}]/dt}{(R_i)^{1/2}} - \frac{k_{p2}}{(2k_{t2})^{1/2}}[\mathrm{R-H_2}]^n = \frac{k_{p1}}{(2k_{t1})^{1/2}}[\mathrm{R-H_1}]^m \tag{13}$$

$$\log\left(\frac{-d[\mathrm{O_2}]/dt}{(R_i)^{1/2}} - \frac{k_{p2}}{(2k_{t2})^{1/2}}[\mathrm{R-H_2}]^n\right) = m\log[\mathrm{R-H_1}] + \log\frac{k_{p1}}{(2k_{t1})^{1/2}} \tag{14}$$

Plotting the left-hand side of the equation against $\log[R\text{-}H_1]$ gives the order of reaction, as the slope, for the component of the autoxidation not associated with the ethylene oxide, $R\text{-}H_2$, substituents.

Experimental Procedures

Materials

PS-80 and PS-20 samples used in all kinetic studies were obtained from Sigma Aldrich as the highest grades available and were labeled as low-peroxide, low-carbonyls and preservative-free. The PS-80 is described as containing ~70% oleic acid, and the iodine value from the certificate of analysis was 22. The certificate of analysis for PS-20 gives an iodine value of 0.9. The water soluble thermal initiator, 2,2′-azobis-2-methyl-propanimidamide, dihydrochloride (AAPH), and the inhibitor, Trolox (6-hydroxy-2,5,7,8-tetramethyl chroma-2-carboxylic acid), were purchased from Sigma Aldrich and produced by the Cayman Chemical Company and TCI America, respectively. Polysorbates were stored at 2–8°C and protected from light while AAPH and Trolox samples were stored at −20°C and protected from light. Kinetic studies were carried out in 100 mM sodium phosphate buffer with 0.1 mM ethylenediaminetetraacetic acid (EDTA) at pH 7.0. EDTA, a metal ion chelating agent, was added as a precaution against metal catalyzed oxidation processes that could interfere with the autoxidation kinetics being studied here (29). Monobasic sodium phosphate monohydrate and anhydrous dibasic phosphate solutions (1 M) used to produce this buffer were USP grade and supplied by Mallinckrodt Chemical. The EDTA was supplied by Teknova as a 0.5 M, pH 8.0, aqueous solution. Water used in buffers was purified using a Milli-Q system (resistivity = 18.2 MΩ.cm at 25°C).

Kinetic Studies

The rate of decomposition of the initiator, AAPH, was evaluated in sodium phosphate buffer at 40°C under three different reaction conditions: AAPH alone, AAPH in the presence of PS-80, and AAPH in the presence of PS-20. A typical experiment was set up in a glass reaction vial with a stir bar. Reaction temperature control (40±0.5°C) and stirring for all studies described here was provided by Pierce Reacti-Therm III equipped with a 600 mL insulated water bath that was protected from light. Decomposition of AAPH was monitored by measuring the loss of the azo-absorption peak at 366 nm in the UV-Vis spectrum by HPLC. A Phenomenex Luna C18, 150 mm×4.6 mm, 5 μm column was used for the separation with mobile phases A and B (A—98:2, H_2O with 0.1% formic acid:MeOH with 0.1% formic acid, B—2:98, H_2O with 0.1% formic acid:MeOH with 0.1% formic acid). The flow rate was 1 mL/min with a 90:10 to 10:90, A:B mobile phase gradient over 8 minutes followed by a 2 min isocratic hold.

An Ocean Optics 1,000 μm fiber optic FOXY-R Oxygen Sensor with MFPF100-1 phase shift fluorescence detector was used to measure autoxidation propagation rates by monitoring head space oxygen consumption. The LED mode was intermittent with a sampling period of 30 s with an integration period of 15 s. Temperature compensation was employed using a vendor-provided multiple temperature calibration curve. The kinetic studies were carried out in air using atmospheric oxygen at 40°C. At the start of each experiment the partial pressure was set at the atmospheric partial pressure of oxygen of 20.9% (22.2 kPa). A typical experiment was set up in a glass reaction vial with a stir bar. The reaction volume was 2 mL with a headspace volume of 2.28 mL to 2.36 mL, depending on the run. The reaction vials were charged with the weighed initiator (AAPH) followed by solutions of polysorbate and Trolox in the reaction buffer (100 mM sodium phosphate buffer with 0.1 mM EDTA at pH 7.0), prepared in volumetric flasks by vortex stirring for 3 min. The atmospheric pressure was recorded at the start of the experiment, and the reaction mixture was sealed using a rubber septum through which the oxygen and temperature probes were introduced to monitor the headspace oxygen concentration and temperature. The reaction vial was then placed in a 40°C water bath, and oxygen pressure and reaction temperature in the headspace were monitored. The ideal gas law was used to determine the moles of O_2 consumed during the reaction from the atmospheric pressure when the vial was sealed, the partial pressure of O_2, and the head space volume and temperature. The inhibition time, τ, was taken as the intercept of the inhibited and uninhibited reaction slopes. Propagation rates (R_p) were determined at <5% conversion of polysorbates and above an O_2 partial pressure of 13.3 kPa, since O_2 is known to become rate limiting below this pressure (22,30). All studies were carried out at total polysorbate concentrations (0.5–5% *w*/*v*) well above their expected critical micelle concentrations (CMC) for PS-20 (0.007%, 25°C) and PS-80 (0.0017%, 25°C) and below their expected cloud points (PS-20: 65–75°C, PS-80: 76°C, 3% (*w*/*v*) solutions in 1 M NaCl) (1,12,31–33). CMC values for PS-20 and PS-80 have only been reported in the literature at 25°C.

Reaction concentrations were corrected for the organic (micellar) volume for the calculation of the reaction rates, chain lengths and oxidizability constants, as is common for surfactant kinetic studies (34). This was required since the polysorbates are not diluted by water, or, in other words, the polysorbate concentration in the micelles was the same as it would be in neat polysorbate. For PS-80 an average molecular mass of 1310 g/mol and a density of 1.064 g/mL, reported by Sigma Aldrich, gave a molar volume of 1.231 L/mol, from which the micellar volume was directly calculated. For PS-20 a density of 1.105 g/mL, as reported by Sigma-Aldrich, was used with a molecular mass of 1128 g/mol.

RESULTS

Determination of Oxidizability Constants

In order to determine initiator efficiency (*e*), rate constants for the decomposition of the azo-initiator (AAPH), k_i, were first determined at 40°C (Table II). The first-order kinetics of AAPH decomposition were monitored by HPLC in aqueous buffer, with and without polysorbates. The rate constants show no significant change in the presence of PS-20 or PS-80 *vs*. buffer alone. This is due to AAPH being present primarily in the aqueous phase, consistent with its hydrophilic nature (34). The average of the six runs, $k_i = (3.62\pm0.18)\times 10^{-6}\ s^{-1}$ at 40°C, is in good agreement with the literature value for the k_i of AAPH ($3.53\times10^{-6}\ s^{-1}$ at 40°C) (35). The value obtained here was used for the determination of *e* (Tables III and IV).

A typical trace showing the amount of O_2 consumed during the autoxidation of PS-80 is presented in Fig. 6. The

Table II. Rate Constants for the Thermal Decomposition of AAPH at 40°C in 100 mM Sodium Phosphate Buffer With 0.1 mM EDTA at pH 7.0

Condition	Run #	Initial AAPH Conc. ($\times 10^{-2}$ M)	Polysorbate Conc. ($\times 10^{-2}$ M)	k_i ($\times 10^{-6}$ s^{-1})
Buffer	1	1.16		3.60
Buffer	2	0.798		3.85
Buffer + PS 20	3	1.16	2.31	3.84
Buffer + PS 20	4	0.809	2.30	3.43
Buffer + PS 80	5	1.15	2.28	3.48
Buffer + PS 80	6	0.815	2.27	3.52
AVERAGE				**3.62±0.18**

trace shows both the Trolox-inhibited and uninhibited stages of the reaction and the trend lines used to calculate τ and R_p. The data for all kinetic runs using simple PS-20 or PS-80 micellar solutions are shown in Table III.

Using Hammond's method, the efficiency (e) of initiator radical escape from the solvent cage was determined from the initiation rate constant k_i and the inhibition time (21). As expected, e was statistically equivalent between the PS-80 and PS-20 systems 0.240±0.012% and 0.242±0.012%, respectively. Again, this is consistent with published results and is explained by the fact that the hydrophilic AAPH initiator decomposes in the aqueous phase regardless of which surfactant is present, PS-20 or PS-80 (34).

The radical chain lengths, ν, determined for these systems (Table III) were relatively short, especially for the autoxidation of PS-20 (19). The primary consequence of these short chain lengths was that the measured rates of oxygen uptake ($d[O_2]/dt$) were a poor approximation of the propagation rates unless the proper correction was made. This correction was necessary since O_2 consumed during the initiation steps, and produced during termination steps, was significant relative to the fraction of O_2 consumed due to propagation of the reaction (Fig. 2). The correction, which was easily applied, is described in Table III and is derived directly from the initiation rate and efficiency at steady state. No correction for the formation of N_2 from initiator was required, since the system was at constant volume and the sensor measures the partial pressure of O_2, not the actual concentration. The average oxidizability of PS-80 is $(1.07\pm 0.19)\times 10^{-2}$ $M^{-1/2}$ $s^{-1/2}$, 2.65 times larger than that of PS-20, which was found to have an average oxidizability constant of $(0.404\pm 0.080)\times 10^{-2}$ $M^{-1/2}$ $s^{-1/2}$ across the concentrations studied.

Determination of Reaction Orders

The reaction order with respect to initiator was investigated using the kinetic order plot method as described above. The data can be found in Table III, runs 2, 3, and 8–17, for which the concentration of AAPH was varied while keeping the PS-80 concentration essentially constant. Trolox concentration was also varied in some reactions to maintain suitable inhibition times for the determination of the efficiency (e). The Trolox concentration had no effect on the measured rate since R_p was measured following the end of the inhibition period. The slope of the kinetic order plot, Fig. 7, yielded a reaction order of 0.56±0.03 for AAPH initiator, consistent with the reaction order of one half required by the kinetic rate law (Eq. 8).

Data for the determination of the reaction order with respect to the concentration of unsaturated substituents can be found in Table IV. The study was performed by varying the relative amounts of PS-20 and PS-80 in the mixed micelles while maintaining a relatively constant total polysorbate concentration (PS-20 + PS-80) in solution. This procedure resulted in a constant concentration of ethylene oxide substitutents across the experimental runs, while the concentration of unsaturated fatty acid ester groups was varied within the micelle. The resulting kinetic order plot, Fig. 8, derived from Eq. 14, required knowledge of the oxidizability constant for the ethylene oxide substituents, $k_{p2}/(2k_{t2})^{1/2}$. For this value, an oxidizability constant of 0.404×10^{-2} $M^{-1/2}$ $s^{-1/2}$ determined from the PS-20 experiments was used (Table III). The reaction order for the ethylene oxide component of the autoxidation, m, in Eq. 14, is assumed to be 1. The slope of the kinetic order plot, Fig. 8, gave a reaction order in unsaturated fatty acid esters of 1.12±0.12. Examination of Eq. 14 also reveals that the oxidizability constant of the unsaturated fatty acid substituents is simply the inverse log of the y-intercept of the kinetic order plot. From Fig. 8, the intercept is 2.09, which gave the oxidizability of the unsaturated fatty acid substituents, $k_{p1}/(2k_{t1})^{1/2}$, as $(0.822\pm 0.130)\times 10^{-2}$ $M^{-1/2}$ $s^{-1/2}$.

DISCUSSION

Due to the well-known ability of polysorbates to promote oxidation of APIs, it is important to assess chemical stability when these excipients are used in formulations (12). It is believed that the propensity of polysorbates to promote API oxidation is due to their own susceptibility to autoxidation, resulting in the formation of high concentrations of ROS, such as peroxyl radicals and peroxides (1,12). The classical oxidizability constant, $k_p/(2k_t)^{1/2}$, isolates the key kinetic terms, the propagation rate constant, k_p, and the termination rate constant, k_t, that define the susceptibility of molecules—polysorbates in this case—to autoxidation and their ability to generate ROS in a system. The oxidizability constant changes as a function of two conditions. First, a compound that is more susceptible to radical chain propagation, by hydrogen atom abstraction or peroxyl radical addition to olefins, will have a larger k_p relative to a less susceptible molecule, and a corresponding increase in the oxidizability constant, O_2 consumption and peroxyl radical and peroxide formation. Second, a smaller k_t is due to slower termination of the autoxidation chain reaction, again resulting in a higher ROS load and a larger oxidizability constant. It is interesting to note that $k_p/(2k_t)^{1/2}$ will be less sensitive to changes in the k_t term than the k_p term due to the square root in the denominator.

Oxidizability constants for the simple PS-20 and PS-80 systems are presented in Table III. As expected, $k_p/(2k_t)^{1/2}$ does not show significant variation across the polysorbate concentration range tested. It has been noted that the two highest oxidizability values for PS-80 were recorded at the lowest concentrations studied, although the highest

Table III. Autoxidation of Polysorbates in Water at 40°C

Condition	Run #	[Polysorbate][a] (× 10^{-2} M)	[AAPH][a] (× 10^{-2} M)	[Trolox][a] (× 10^{-5} M)	Inhibition time (× 10^{3} s)	R_i[a] (× 10^{-8} M s−1)	R_i[b] (× 10^{-7} M s−1)	e	$d[O_2]/dt$[b] (× 10^{-6} M s^{-1})	$d[O_2]/dt$[b,c] (× 10^{-6} M s^{-1})	ν[b]	Oxidizability $k_p/(2k_t)^{1/2}$ [b] (× 10^{-2} $M^{-1/2}$ $s^{-1/2}$)
5% PS-80	1	3.73	1.17	9.07	9.25	1.96	4.27	0.231	6.13	5.91	13.8	1.11
3% PS-80	2	2.20	1.16	9.08	9.04	2.01	7.41	0.240	6.25	5.88	7.9	0.84
3% PS-80	3	2.26	1.13	9.21	9.13	2.02	7.25	0.246	7.27	6.91	9.5	1.00
2% PS-80	4	1.52	1.15	9.21	9.46	1.95	10.4	0.233	7.86	7.34	7.0	0.89
2% PS-80	5	1.48	1.18	9.41	9.75	1.93	10.6	0.227	11.5	11.0	10.4	1.32
1% PS-80	6	0.73	1.16	9.21	9.07	2.03	22.5	0.242	18.3	17.2	7.6	1.41
0.5% PS-80	7	0.36	1.15	9.07	9.66	1.88	42.3	0.225	27.4	25.3	6.0	1.52
3% PS-80	8	2.28	0.14	2.37	18.7	0.25	0.90	0.245	2.39	2.35	26.0	0.96
3% PS-80	9	2.27	0.14	2.31	19.5	0.24	0.84	0.228	2.32	2.28	27.0	0.97
3% PS-80	10	2.25	0.29	9.22	36.0	0.51	1.85	0.242	3.26	3.16	17.1	0.91
3% PS-80	11	2.22	0.29	9.24	38.4	0.48	1.76	0.225	3.42	3.33	18.9	0.98
3% PS-80	12	2.23	0.56	9.32	18.3	1.02	3.71	0.250	4.90	4.71	12.7	0.95
3% PS-80	13	2.24	0.55	9.86	20.2	0.98	3.54	0.244	4.65	4.48	12.6	0.93
3% PS-80	14	2.22	1.53	9.24	6.89	2.68	9.83	0.243	9.98	9.49	9.6	1.18
3% PS-80	15	2.28	1.50	9.16	6.51	2.81	10.0	0.259	9.69	9.19	9.2	1.13
3% PS-80	16	2.25	2.29	9.62	4.36	4.42	15.9	0.266	10.7	9.86	6.2	0.96
3% PS-80	17	2.20	2.25	18.2	9.25	3.94	14.6	0.242	12.0	11.3	7.8	1.15
AVERAGE								**0.240±0.012**				**1.07±0.19**
4% PS-20	1	3.44	1.15	9.04	9.48	1.91	5.43	0.228	2.56	2.29	4.2	0.317
2.6% PS-20	2	2.24	1.16	13.8	13.5	2.05	8.98	0.244	4.61	4.16	4.6	0.448
2.6% PS-20	3	2.23	1.13	9.27	9.66	1.92	8.41	0.235	3.61	3.19	3.8	0.355
1.5% PS-20	4	1.31	1.21	9.32	8.73	2.14	16.0	0.244	6.23	5.43	3.4	0.439
0.7% PS-20	5	0.61	0.57	4.56	8.33	1.09	17.6	0.264	5.31	4.43	2.5	0.341
0.5% PS-20	6	0.43	0.58	4.58	9.08	1.01	23.1	0.239	8.98	7.83	3.4	0.526
AVERAGE								**0.242±0.012**				**0.404±0.08**

[a] Calculated using total solution volume
[b] Calculated using total micellar volume
[c] Rates have been corrected for the absorption of O_2 by the initiator and the O_2 evolved in chain termination by substraction of ek_i[AAPH] from the measured rates

Table IV. Autoxidation of PS-20 and PS-80 Mixed Micelles in Water at 40°C

Mole fraction PS-80	Run #	([PS-20]+[PS-80])[a] ($\times 10^{-2}$ M)	[AAPH][a] ($\times 10^{-2}$ M)	[Trolox][a] ($\times 10^{-5}$ M)	Inhibition time ($\times 10^{3}$ s)	R_i[a] ($\times 10^{-8}$ M s^{-1})	R_i[b] ($\times 10^{-7}$ M s^{-1})	e	d[O_2]/dt[b] ($\times 10^{-6}$ M s^{-1})	d[O_2]/dt[b,c] ($\times 10^{-6}$ M s^{-1})	v[b]	Oxidizability $k_p/(2k_t)^{1/2}$[b] ($\times 10^{-2}$ M$^{-1/2}$ s$^{-1/2}$)	$\log(R_p/(R_i)^{1/2}$ -Oxidizability$_{(PS\text{-}20)}$ $\times$ ([PS-20]+[PS-80])]
1.00	1	2.20	1.16	9.08	9.04	2.01	7.41	0.240	6.25	5.88	7.9	0.84	−2.42
1.00	2	2.26	1.13	9.21	9.13	2.02	7.25	0.246	7.27	6.91	9.5	1.00	−2.29
0.802	3	2.22	1.17	9.13	8.84	2.06	7.81	0.244	8.70	8.31	10.7	1.12	−2.20
0.606	4	2.26	1.16	9.28	9.52	1.95	7.51	0.231	7.13	6.76	9.0	0.90	−2.34
0.604	5	2.23	1.15	9.58	9.50	2.02	7.87	0.242	6.96	6.57	8.3	0.85	−2.38
0.401	6	2.24	1.17	9.08	9.37	1.94	7.82	0.229	6.66	6.27	8.0	0.78	−2.43
0.296	7	2.25	1.14	9.86	10.8	1.82	7.47	0.221	5.85	5.47	7.3	0.69	−2.54
0.199	8	2.26	1.17	9.37	9.59	1.96	8.16	0.231	5.06	4.65	5.7	0.55	−2.78
0.192	9	2.26	1.15	9.41	9.83	1.92	7.99	0.230	4.59	4.19	5.2	0.50	−2.92
0.147	10	2.25	1.15	9.35	9.57	1.95	8.27	0.234	4.47	4.06	4.9	0.47	−3.03
0.139	11	2.33	1.15	9.24	9.51	1.94	7.93	0.234	4.11	3.72	4.7	0.44	−3.19
0.095	12	2.26	1.15	9.58	9.79	1.96	8.33	0.236	4.02	3.61	4.3	0.41	−3.41

[a] Calculated using total solution volume
[b] Calculated using total micellar volume
[c] Rates have been corrected for the absorption of O_2 by the initiator and the O_2 evolved in chain termination by substraction of ek_i[AAPH] from the measured rates

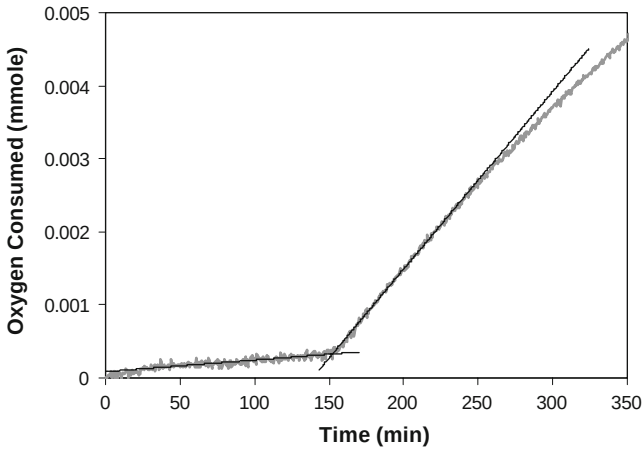

Fig. 6. Autoxidation of 3% (22.6 mM) PS-80 in aqueous buffer with 11.3 mM AAPH and 92.1 μM Trolox showing trend lines for extrapolation.

oxidizability constant is just outside of two standard deviations. A similar observation can be made for PS-20, but in this case the second lowest oxidizability was also recorded for the second lowest concentration (0.7% PS-20). Due to the lack of a consistent trend and the fact that the highest variability will occur in the kinetics for the slowest reactions, it is likely that the observed variation reflects the expected data distribution. The data set also includes a variety of different AAPH concentrations, resulting in a 12.6-fold range in the initiation rate without affecting the oxidizability constants, and showing that the procedure effectively isolated the initiation rate terms from k_p and k_t. Likewise, a range of Trolox concentrations were used without effect on the measured oxidizabilities. The oxidizability constants for PS-80 and PS-20 were found to be $(1.07\pm 0.19)\times 10^{-2}$ $M^{-1/2}$ $s^{-1/2}$ and $(0.404\pm 0.080)\times 10^{-2}$ $M^{-1/2}$ $s^{-1/2}$, respectively. These relatively low values are similar to those

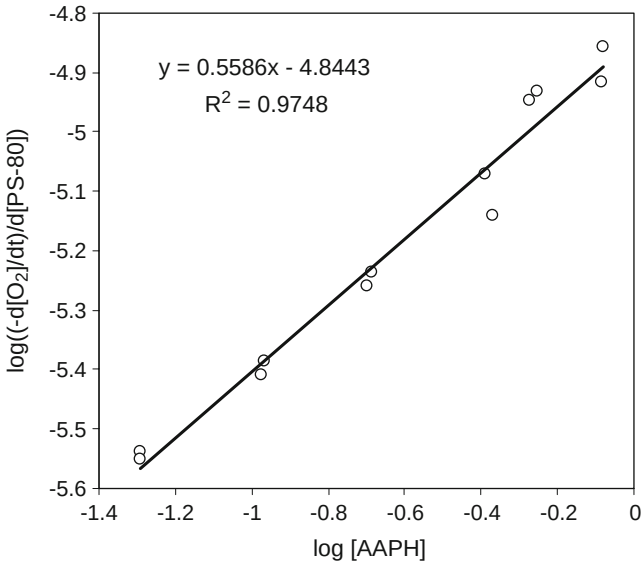

Fig. 7. Kinetic order plot of O_2 consumption with concentration of initiator, AAPH, for the autoxidation of PS-80 micelles.

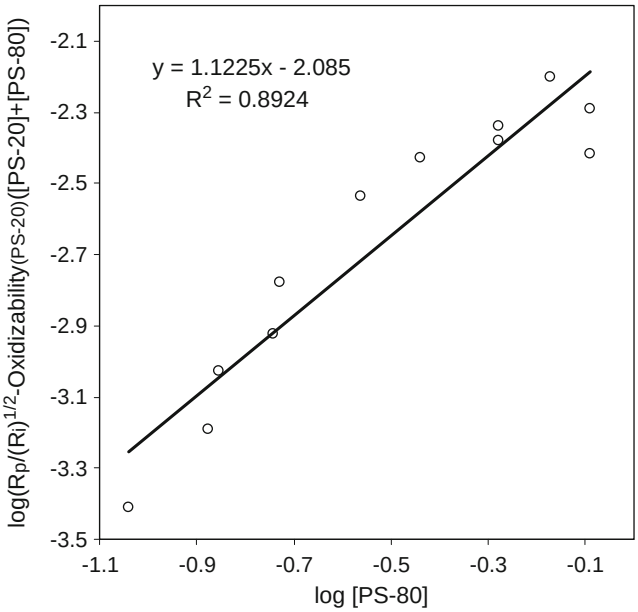

Fig. 8. Kinetic order plot of O_2 consumption with the concentration of fatty acid ester substituents in mixed micelles of PS-80 and PS-20.

obtained for the autoxidation of egg lecithin, a monounsaturated fatty acid ester of phosphatidylcholine, in aqueous bilayer dispersions. Using a similar technique as described here, the oxidizability constant for egg lecithin has been determined in aqueous NaCl at 30°C to be 1.65×10^{-2} $M^{-1/2}$ $s^{-1/2}$ (19,36). The oxidizability of PS-80 is 2.65 times that of PS-20, indicating that PS-80 is significantly more susceptible to autoxidation than PS-20. The implication is that PS-80 has the potential to generate high concentrations of reactive oxygen species faster than PS-20, making it a greater liability for the formulation of compounds that undergo oxidative degradation.

Now that an increased oxidative liability for PS-80 over PS-20 has been identified and quantified, it is important to focus on identifying its source. If the autoxidation of polysorbates were only linked to degradation of the ethylene oxide polymer subunits, the oxidizability constants of PS-80 and PS-20 would have been expected to be the same, since each molecule has the same number, 20, of repeat ethylene oxide subunits. Based on the enthalpies of reaction estimated in the introduction, it is expected that the unsaturated fatty acid ester substituents may be far more susceptible to autoxidation than the ethylene oxide groups. However, in order for oxidation of the unsaturated groups to contribute significantly to the overall reaction, or even just compete with the ethylene oxide substituents, a statistical factor must also be overcome. For example, an examination of the general PS-80 structure reveals that the sorbitan ring and the ethylene oxide substituents contribute 22-fold excess of H-atom abstraction sites (88 **H**-C-O sites) compared to the oleic fatty acid ester substituent (4 **H**-C-CH = CH- sites), the primary fatty acid component of PS-80. Is the predicted susceptibility of the unsaturated groups sufficient to overcome this statistical factor and account for the additional reactivity of PS-80?

To investigate the possibility that the unsaturated fatty acid ester substituents account for the additional reactivity of PS-80, the component of the reaction associated with the polyethylene oxide groups was isolated, and the dependence of the reaction on the unsaturated substituents was determined. This was accomplished using mixed micelles of PS-80 and PS-20 to vary the concentration of unsaturated fatty acid esters within the micelles while holding the total polyethylene oxide concentration constant and analyzing the resulting propagation rates using a modified van't Hoff kinetic order plot approach, according to Eq. 14 (28). The slope of the kinetic order plot, 1.12±0.12, Fig. 8, reveals that the non-polyethylene oxide component of the oxidation of PS-80 was first-order with respect to the unsaturated fatty acid ester substituents. The reaction order relative to AAPH initiator was also examined to help verify the validity of the kinetic procedures being used and to support the proposed autoxidation mechanism for PS-80. The kinetic order plot, Fig. 7, gives a reaction order of 0.56±0.03 and is consistent with the half-order dependence required for AAPH based on the classical rate law, Eq. 8. Under conditions where the oxidation is independent of the O_2 concentration (partial pressure >13.3 kPa) the key criteria for determining if the kinetics are consistent with autoxidation are, first, that the reaction rate is half-order with respect to the initiator concentration, since one mole of azo-initiator yields two moles of radicals, and, second, that the reaction is first-order with respect to substrate (R-H) concentration (21,22). The first-order dependence on the concentration of PS-80 unsaturated side chains and the half-order dependence on the initiator, AAPH, fulfill these two criteria and strongly support a role for fatty acid ester substituents in the autoxidation of PS-80.

The magnitude of the contribution of the fatty acid ester substituents to the autoxidation of PS-80 was assessed based on further analysis of the kinetic order plot for the unsaturated substituents (Fig. 8). From the intercept, the oxidizability of the unsaturated fatty acid substituents, $k_{p1}/(2k_{t1})^{1/2}$, was calculated to be $(0.822\pm0.13)\times10^{-2}$ $M^{-1/2}$ $s^{-1/2}$. The total oxidizability constant, $k_p/(2k_t)^{1/2}$, of PS-80 was determined from data in Table III to be $(1.07\pm0.19)\times 10^{-2}$ $M^{-1/2}$ $s^{-1/2}$. It is encouraging that the oxidizability constant for the unsaturated substituents is very close to the difference in the oxidizability constants for PS-80 and PS-20, but it should be noted that it is not absolutely correct to subtract oxidizability constants ($k_p/(2k_t)^{1/2}$) in this manner due to the difference in the denominator, $(2k_t)^{1/2}$ term, for different substituents. However, based on the oxidizability constants for PS-20 and the unsaturated substituents, it is clear that the unsaturated fatty acid ester substituents not only participated in the autoxidation of PS-80, but were twice as reactive as the ethylene oxide moieties and would be expected to account for 2/3 of the total autoxidation of PS-80. As a result, the unsaturated fatty acid esters would be expected to be responsible for the bulk of the ROS generated in a PS-80 solution. This result is consistent with the expected relative enthalpies of reaction discussed in the introduction. Insight into the roles of the different unsaturated fatty acids can also be gained from a comparison of the oxidizability constants determined here to the available kinetic information for unsaturated fatty acid and ether models. Data has been tabulated for the propagation rate

constants and the oxidizabilities of ethers and fatty acids (27). Due to differences in experimental conditions used to determine propagation rate constants, the importance of the termination rate constants in the observed autoxidation rates, and the necessity to account for additional reaction pathways (e.g. addition to double bonds), the discussion will be limited to the $k_p/(2k_t)^{-1/2}$ data, which inherently accounts for these important factors. The relative oxidizabilities, at 30°C, of pure methyl oleate (8.9×10^{-4} $M^{-1/2}$ $s^{-1/2}$), methyl linoleate (2.1×10^{-2} $M^{-1/2}$ $s^{-1/2}$), and methyl linolenate (3.9×10^{-2} $M^{-1/2}$ $s^{-1/2}$) esters are 1 : 24 : 44, respectively (37). Considerable variation is apparent in the reported oxidizabilities of different saturated ethers, due in part to the importance of intramolecular propagation reactions and intermolecular termination reactions specific to ethers (38,39). As a result, n-butyl ether with an oxidizability of 1.0×10^{-4} $M^{-1/2}$ $s^{-1/2}$ is the most suitable acyclic unsaturated ether model available with methylene groups in the reactive position (27,39). Based on this value and estimating that PS-80 has approximately 22 times the number of reactive ether sites of n-butyl ether, resulting in a 22-fold relative increase in k_p, the oxidizability constant representing the ethylene oxide substituents can be estimated to be 2.2×10^{-3} $M^{-1/2}$ $s^{-1/2}$ ($22\times(1.0\times10^{-4}$ $M^{-1/2}$ $s^{-1/2}$)) (37,40). Although this analysis does not account for environmental factors, such as the different media, comparison of this value to the reported oxidizability of methyl oleate (8.9×10^{-4} $M^{-1/2}$ $s^{-1/2}$) does suggest that oleate ester component of a given PS-80 molecule would be about 2.5 times less reactive than the ethylene oxide substituents, and would not be expected to overcome the 22-fold statistical factor. However, the linoleate and linolenate ester groups are expected to be 9.5 and 18 times more reactive for a given molecule than the ethylene oxide components. It seems likely the minor di- and tri-unsaturated fatty acid ester components are making a significant contribution to the overall oxidation of PS-80 that results in the domination of the oxidation kinetics over ethylene oxide autoxidation. In fact, the unsaturated fatty acid oxidizability value of $(0.822\pm0.13)\times10^{-2}$ $M^{-1/2}$ $s^{-1/2}$ (40°C), calculated here from the van't Hoff analysis, lies inside the reported oxidizability range for methyl oleate, methyl linoleate, and methyl linolenate reported at 30°C and could easily be the product of the known oxidizability constants of the different fatty acid ester substituents. The PS-80 used in this study from Sigma-Aldrich (~70% oleic acid) has an average of 1.14 unsaturated bonds per polysorbate molecule as determined from its iodine value of 22 (41). This value is consistent with the presence of some di- and tri-unsaturated fatty acid esters on the order of the concentrations defined by the EU specification (Table I), although the exact composition is not known (10).

The data provides strong evidence that PS-80 not only undergoes autoxidation, but that the unsaturated fatty acid ester groups account for 2/3 of the reactivity. With this information in hand, it is worth making a brief comment about the autoxidation of PS-20. As stated earlier, PS-20 and PS-80 are generally sold as mixtures, varying in their fatty acid ester substituents (7–9). The PS-20 sample has an iodine value of 0.9, giving an average of 0.04 unsaturated fatty acid groups per polysorbate, indicating a 28-fold lower double bond concentration than the PS-80 sample (41). It has been assumed that the oxidizability constant measured for PS-20 ($(0.404\pm0.080)\times10^{-2}$ $M^{-1/2}$ $s^{-1/2}$) was due to the polyethylene glycol groups, but could the 4% of unsaturated groups actually make a dominant contribution to this value? If the observed unsaturation was due entirely to the most reactive unsaturated fatty acid ester present in PS-20, linoleate, then the total concentration of linoleate would be 2%, and the potential oxidizability can be estimated from the literature value for methyl linoleate ($2\%\times(2.1\times10^{-2}$ $M^{-1/2}$ $s^{-1/2}$)) giving an oxidizability of 4.2×10^{-4} $M^{-1/2}$ $s^{-1/2}$ (10). This upper limit is an order of magnitude lower than the measured PS-20 oxidizability and indicates the unsaturated fatty acids present in the PS-20 sample used here could not account for the measured oxidizability constant. This supports the contention that the autoxidation of the polyethylene glycol groups is the major contribution to the oxidation of PS-20, consistent with the studies by Donbrow on PS-20 and other non-ionic surfactants (12,23). A more detailed study of the classical kinetics of PS-20 oxidation is being executed to study the contribution of ethylene oxide substituents. The PS-20 system cannot be treated exactly as was done here for PS-80 due to the relatively slow reaction and the challenge of varying the ethylene oxide substituent's concentration in a polysorbate micelle.

CONCLUSION

The kinetic results for PS-80 show that it is significantly more susceptible to oxidation than PS-20, and this difference in reactivity cannot be explained solely based on the reactivity of the polyethylene oxide substituents alone. PS-80 oxidation kinetics followed the classical autoxidation rate law, and it was shown for the first time that the additional oxidative reactivity is dependent on, and first-order in, the unsaturated fatty acid ester substituents. In fact, based on the oxidizability constants for PS-20, PS-80, and the estimated value for the unsaturated substituents alone, 2/3 of the autoxidation is due to the unsaturated fatty acid ester groups. These results indicate that additional care should be taken when using PS-80 in formulations, and suggests possible strategies to avoid oxidation of formulated APIs. Successful options for minimizing oxidative degradation of pharmaceuticals exposed to autoxidative environment presented by polysorbates include protection from heat and light, which can initiate the chain reaction; the use of radical chain terminating antioxidants; scavenging peroxides; and protection from oxygen using sealed containers or nitrogen filled head space (2,13,17,29). The results presented here suggest that substituting with polysorbates that do not have unsaturated fatty acid esters as a primary component could also help to control oxidation. It seems that PS-20 would be an obvious alternative, containing ≤14% unsaturated fatty acids and having similar physicochemical properties, including CMC values (PS-20: 0.007%, PS-80: 0.0017%) and cloud points (PS-20: 65–75°C, PS-80: 76°C, 3% (*w*/*v*) solutions in 1 M NaCl) (1,12,31–33). Alternatively, if the use of PS-80 is desired, it is possible that significant improvement in the oxidative stability characteristics of these formulations may be achieved by employing PS-80 samples designed to be low in di- and tri-unsaturated fatty acid esters, since, based on the initial analysis presented here, these substituents appear to be the most serious offenders. While these alternative polysorbates still meet European and United States Pharmacopoeias' specifications, substituting polysorbates with different fatty

acid compositions may have unforeseen consequences for the physicochemical performance of a formulation that should be carefully evaluated (10,11).

Current efforts in our group are focused on a number of areas, including verification of the reaction order for polyethylene oxide substituents in a micellar environment. As was indicated above, this is challenging due to the relatively slow autoxidation of PS-20 and the difficulty in varying the polyethylene oxide concentration in a polysorbate micelle. An assessment of the oxidizability of polysorbates of different ages, grades and from different manufactures may also provide important information for formulators.

ACKNOWLEDGEMENTS

The authors would like to thank Amgen Inc. for funding, Jodi Liu for discussions regarding statistical analysis of the data, and the reviewers for critical reading of this manuscript and their suggestions, especially to highlight the potential importance of linoleic and linolenic fatty acid ester substituents. J. Y. thanks Amgen Inc. for a summer graduate internship.

REFERENCES

1. Kerwin BA. Polysorbates 20 and 80 used in the formulation of protein biotherapeutics: structure and degradation pathways. J Pharm Sci. 2008;97:2924–35.
2. Ha E, Wang W, Wang YJ. Peroxide formation in polysorbate 80 and protein stability. J Pharm Sci. 2002;91:2252–64.
3. Nema S, Washkuhn RJ, Brendel RJ. Excipients and their use in injectable products. J Pharm Sci Technol. 1997;51:166–71.
4. Strickley RG. Solubilizing excipients in oral and injectable formulations. Pharm Res. 2004;21:201–30.
5. Neervannan S. Preclinical formulations for discovery and toxicology: physicochemical challenges. Expert Opin Drug Metab Toxicol. 2006;2:714–31.
6. Rowe RC, Sheskey PJ, Weller PJ, editors. Handbook of pharmaceutical excipients. London: Pharmaceutical Press and the American Pharmaceutical Association; 2003.
7. Brandner JD. The composition of Nf-defined emulsifiers: Sorbitan monolaurate, monopalmitate, monostearate, monooleate, polysorbate 20, polysorbate 40, polysorbate 60, and polysorbate 80. Drug Dev Ind Pharm. 1998;24:1949–054.
8. Ayorinde FO, Gelain SV, James J, Johnson H, Wan LW. Analysis of some commercial polysorbate formulations using matrix-assisted laser desorption/ionization time-of-flight mass spectrometry. Rapid Commun Mass Spectrom. 2000;14:2116–24.
9. Frison-Norrie S, Sporns P. Investigating the molecular heterogeneity of polysorbate emulsifiers by Maldi-Tof Ms. J Agric Food Chem. 2001;49:3335–40.
10. European Pharmacopoeia. On-line 5th edition: European Directorate for the Quality of Medicines and Healthcare. 2007.
11. The United States Pharmacopeia; the National Formulary. On-line USP 31-NF 26 edition: United States Pharmacopeial Convention. 2008.
12. Donbrow M, Azaz E, Pillersdorf A. Autoxidation of polysorbates. J Pharm Sci. 1978;67:1676–81.
13. Waterman KC, Adami RC, Alsante KM, Hong J, Landis MS, Lombardo F, *et al.* Stabilization of pharmaceuticals to oxidative degradation. Pharm Dev Technol. 2002;7:1–32.
14. Jaeger J, Sorensen K, Wolff SP. Peroxide accumulation in detergents. J Biochem Biophys Methods. 1994;29:77–81.
15. Lever M. Peroxides in detergents as interfering factors in biochemical analysis. Anal Biochem. 1977;83:274–84.
16. Magill A, Becker AR. Spectrophotometric method for quantitation of peroxides in Sorbitan monooleate and monostearate. J Pharm Sci. 1984;73:1663–4.
17. Segal R, Azaz E, Donbrow M. Peroxide removal from non-ionic surfactants. J Pharm Pharmacol. 1979;31:39–40.
18. Harmon PA, Kosuda K, Nelson E, Mowery M, Reed RA. A novel peroxy radical based oxidative stressing system for ranking the oxidizability of drug substances. J Pharm Sci. 2006;95:2014–28.
19. Barclay LRC, Ingold KU. Autoxidation of biological molecules. 2. The autoxidation of a model membrane. A comparison of the autoxidation of egg lecithin phosphatidylcholine in water and in chlorobenzene. J Am Chem Soc. 1981;103:6478–85.
20. Betts J. The kinetics of hydrocarbon autoxidation in the liquid phase. Quartlery Rev Chem Soc. 1971;25:265–88.
21. Boozer CE, Hammond GS, Hamilton CE, Sen JN. Air oxidation hydrocarbons. II. The stoichiometry and fate of inhibitors in benzene and chlorobenzene. J Am Chem Soc. 1955;77:3233–7.
22. Ingold KU. Peroxy radicals. Acc Chem Res. 1969;2:1–9.
23. Donbrow M, Hamburger R, Azaz E, Pillersdorf A. Development of acidity in non-ionic surfactants: formic and acetic acid. The Analyst. 1978;103:400–2.
24. Donbrow M. Stability of the polyoxyethylene chain. In: Schick MJ, editor. Nonionic surfactants: physical chemistry. New York: Marcel Dekker; 1987. p. 1060–5.
25. Yin H, Porter NA. New insights regarding the autoxidation of polyunsaturated fatty acids. Antioxid Redox Signal. 2004;7:170–84.
26. Lide DR, editor. CRC handbook of chemistry and physics. New York: CRC Press LLC; 2006–2007.
27. Denisov ET, Afanas'ev IB. Oxidation and antioxidants in organic chemistry and biology, edn. New York: CRC; 2005.
28. Steinfeld JI, Francisco JS, Hase WL. Chemical kinetics and dynamics, edn. Englewood Cliffs: Prentice Hall; 1989.
29. Hovorka SW, Schöneich C. Oxidative degradation of pharmaceuticals: theory, mechanisms and inhibition. J. Pharm. Sci. 2001;90.
30. Bateman L. Olefin oxidation. Quart Revs Chem Soc. 1954;8:147–67.
31. Helenius A, McCaslin DR, Fries E, Tanford C. Properties of detergents. Methods Enzymol. 1979;56:734–49.
32. Mittal KL. Determination of CMC of polysorbate 20 in aqueous solution by surface tension method. J Pharm Sci. 1972;61:1334–5.
33. Patist A, Bahagwat SS, Penfield KW, Aikens P, Shah DO. On the measurement of critical micelle concentrations of pure and technical-grade nonionic surfactants. J Surfactants Deterg. 2000;3:53–8.
34. Barclay LRC, Locke SJ, MacNeil JM, VanKessel J, Burton GW, Ingold KU. Autoxidation of micelles and model membranes. Quantitative kinetic measurements can be made by using either water-soluble or lipid-soluble initiators with water-soluble or lipid-soluble chain-breaking antioxidants. J Am Chem Soc. 1984;106:2479–81.
35. Dekking HGG. Propagation of vinyl polymers on clay surfaces. I. Preparation, structure, and decomposition of clay initiators. J Appl Polym Sci. 1965;9:1641–51.
36. Barclay LRC, Ingold KU. Autoxidation of a model membrane. A comparison of the autoxidation of egg lecithin phosphatidylcholine in water and in chlorobenzene. J Am Chem Soc. 1980;102:7792–4.
37. Howard JA, Ingold KU. Absolute rate constants for hydrocarbon autoxidation. Vi. Alkyl aromatic and olefinic hydrocarbons. Can J Chem. 1967;45:793–802.
38. Howard JA, Ingold KU. Absolute rate constants for hydrocarbon autoxidation. XVII. The oxidation of some cyclic ethers. Can J Chem. 1969;47:3809–15.
39. Howard JA, Ingold KU. Absolute rate constants for hydrocarbon autoxidation. XVIII. Oxidation of some acyclic ethers. Can J Chem. 1969;48:873–80.
40. Benson SW. Thermochemical kinetics, methods for the estimation of thermochemical data and rate parameters. 2nd ed. New York: Wiley; 1976.
41. Ng S, Gee PT. Determination of iodine value of palm and palmkernel oil by Carbon-13 nuclear magnetic resonance spectroscopy. Eur J Lipid Sci Technol. 2001;103:223–7.